Macromolecular Bioscience
www.mbs-journal.de

Mechanically Robust Electrospun Hydrogel Scaffolds Crosslinked via Supramolecular Interactions

*Björne B. Mollet, Sergio Spaans, Parinaz Goodarzy Fard, Noortje A. M. Bax, Carlijn V. C. Bouten, and Patricia Y. W. Dankers**

One of the major challenges in the processing of hydrogels based on poly(ethylene glycol) (PEG) is to create mechanically robust electrospun hydrogel scaffolds without chemical crosslinking postprocessing. In this study, this is achieved by the introduction of physical crosslinks in the form of supramolecular hydrogen bonding ureido-pyrimidinone (UPy) moieties, resulting in chain-extended UPy-PEG polymers (CE-UPy-PEG) that can be electrospun from organic solvent. The resultant fibrous meshes are swollen in contact with water and form mechanically stable, elastic hydrogels, while the fibrous morphology remains intact. Mixing up to 30 wt% gelatin with these CE-UPy-PEG polymers introduce bioactivity into these scaffolds, without affecting the mechanical properties. Manipulating the electrospinning parameters results in meshes with either small or large fiber diameters, i.e., 0.63 ± 0.36 and 2.14 ± 0.63 µm, respectively. In that order, these meshes provide support for renal epithelial monolayer formation or a niche for the culture of cardiac progenitor cells.

1. Introduction

For regenerative medicine and tissue engineering purposes a diversity of biomaterial hydrogels, ranging from natural to synthetic, have been described and studied,[1–6] each with their specific advantages and limitations. Hydrogels of natural origin, such as collagen or its denatured form gelatin, hyaluronic acid, and matrigel, a widely applied commercial extracellular matrix (ECM) mimic, all provide biological environments that promote cellular survival and interaction with cells.[7] However, the variable composition of these materials, and their complex and not-well understood interactions with cells, challenge controlled application. In addition, origin-related safety concerns put constraints on their use in the medical field.[8] On top of that, the possibility to tune the mechanical or topological properties of these molecularly predefined hydrogels is limited. Inert synthetic hydrogels, on the other hand, allow adjustable composition and hence predictable and tunable properties. However, synthetic materials lack bioactive cues for engagement of specific interaction with cells. To bridge the gap between natural and synthetic hydrogels, researchers have simply mixed hydrogel components of natural and synthetic origin to achieve hybrid hydrogels with synergistic effects.[9–11]

To enable the formation of structurally defined, freestanding meshes, the hydrogel system must allow processing and acquire mechanically robust properties. Electrospinning is an attractive processing technique for the formation of fibrous meshes. By controlling fiber diameter, the pore size can be tuned. This allows the formation of scaffolds either distinctly suitable to function as 2D support, or 3D scaffolds that allow cell infiltration. Electrospinning of natural,[12,13] synthetic,[14–17] and hybrid[18] hydrogelators has been performed extensively. However, all these biomaterials require chemical crosslinking post-electrospinning to prevent complete dissolution or fast degradation of the nano-to-micro fibrous structures in aqueous environments and/or to improve poor mechanical properties. A hydrogel material that forms strong physical crosslinks could circumvent the need of chemical crosslinking, while retaining the opportunity for processing.

Here we demonstrate the use of a supramolecular hydrogelator based on poly(ethylene glycol) (PEG) with multiple ureido-pyrimidinone (UPy)-moieties in the backbone,[19] electrospun into mechanically strong, microfibrous meshes (**Figure 1**A). While this chain-extended UPy-PEG (CE-UPy-PEG) has a nearly identical chemical composition compared to its telechelic analogues, it exhibits completely different, exceptional mechanical properties.[20–23] In the dry state, this supramolecular polymer forms a tough material with shape memory properties, whereas in the hydrated state a strong and highly elastic hydrogel is formed.[19] In the equilibrium hydrated state, the bulk hydrogel (with 10 kg mol^{-1} PEG-block) contains ≈85 wt% water. This hydrogel material showed nearly perfect strength recovery even at large deformation (>300%).[19] Hence, the increased chain length, realized through chain-extension, and the ability to form physical crosslinks substantially enhanced the strength, ductility, and stability of this material in water. Importantly, no chemical crosslinking is needed to achieve these remarkable material properties while at the

Dr. B. B. Mollet, P. Goodarzy Fard, Dr. P. Y. W. Dankers
Department of Biomedical Engineering
Laboratory of Chemical Biology
Institute for Complex Molecular Systems
Eindhoven University of Technology
P.O. Box 513, 5600 MB Eindhoven, The Netherlands
E-mail: p.y.w.dankers@tue.nl
S. Spaans, Dr. N. A. M. Bax, Prof. C. V. C. Bouten, Dr. P. Y. W. Dankers
Department of Biomedical Engineering
Laboratory for Cell and Tissue Engineering
Institute for Complex Molecular Systems
Eindhoven University of Technology
P.O. Box 513, 5600 MB Eindhoven, The Netherlands

DOI: 10.1002/mabi.201700053

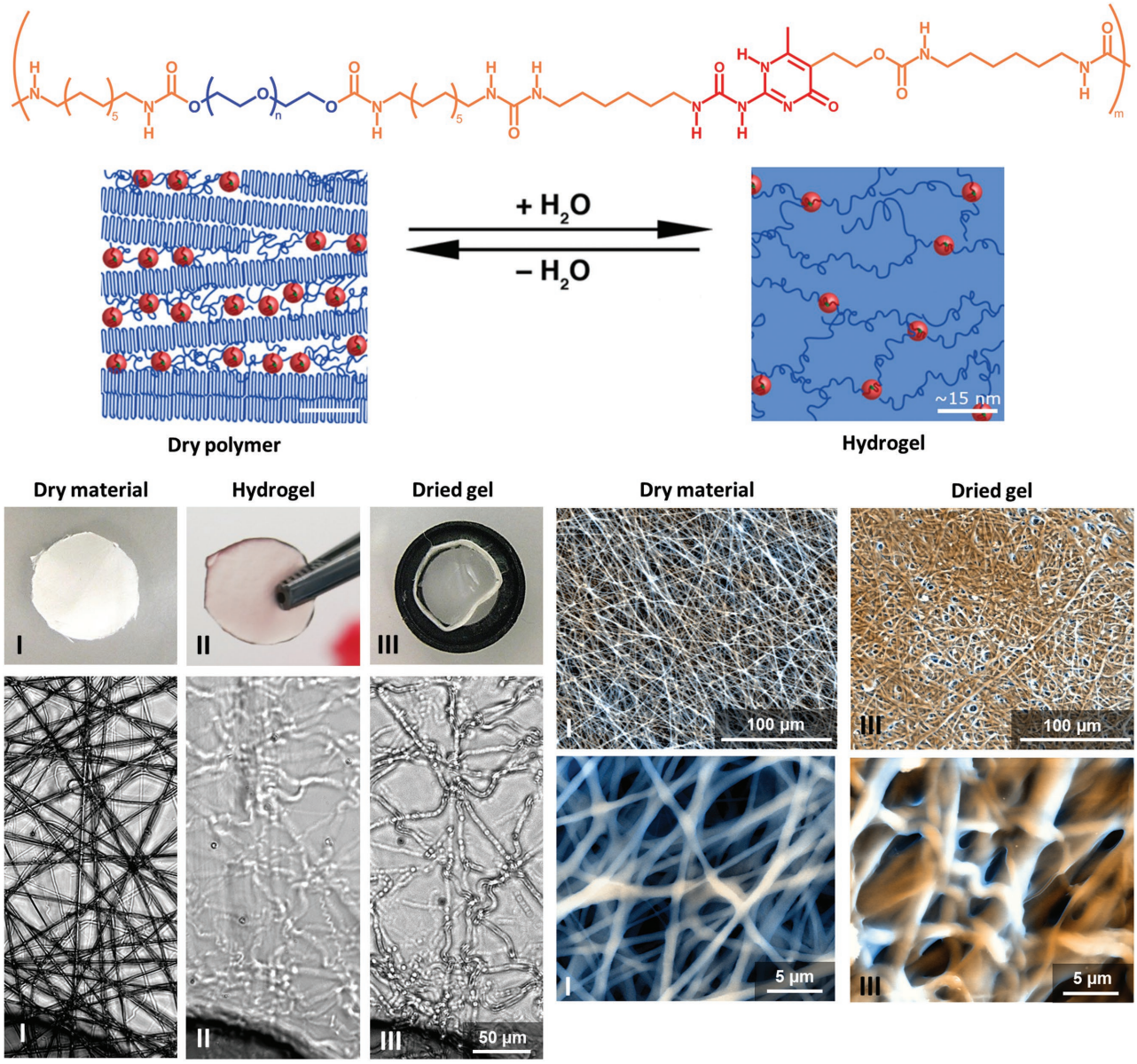

Figure 1. Formation of electrospun CE-UPy-PEG scaffolds in aqueous environments. Chemical structure of CE-UPy-PEG and the effect of water on the nanometer-scale polymer structure, scale bars represent ≈15 nm. Photographs of a stand-alone electrospun mesh and phase contrast micrographs of a thin layer of electrospun microfibers on a glass substrate as-spun (state I) dry material, (state II) as a hydrogel after addition of cell culture media containing phenol red and (state III) dehydrated gel. Scale bars of the photographs and for the micrographs are 5 mm and 50 µm, respectively. Scanning electron micrographs show the microfibrous morphology of electrospun CE-UPy-PEG meshes as-spun (state I) dry material from a solution in HFIP and (state III) after hydration and subsequent drying. Scale bars of the upper micrographs and the lower micrographs are 100 and 5 µm, respectively.

same time the physical crosslinks, formed by hydrogen-bonding between UPy-dimers, are reversible by nature. As such, these links can be dissociated and reformed as desired in a controlled fashion, offering attractive processing opportunities.

Based on these properties, CE-UPy-PEG was hypothesized to be well-suited as hydrogel scaffold material for tissue engineering applications. To induce a cell adhesive character to the bio-inert CE-UPy-PEG, mixing with a bioactive natural hydrogel component was performed. For this purpose gelatin was chosen, due to its compatibility with electrospinning processes.[24–26] By incorporation of gelatin in the electrospinning process, we demonstrate the use of this hydrogel scaffold to support the formation of renal monolayers and as a cardiac progenitor cell niche.

2. Experimental Section

2.1. Materials

CE-UPy-PEG with $M_{n,PEG}$ = 10 kg mol^{-1} was synthesized as previously described.[19] As a consequence of the high polydispersity index (PDI >3) the number of repeats, or UPy-functionalities, per macromolecular monomer was estimated to be around 50 repeats on average based on average molecular weight determined by gas permeation chromatography (GPC).

Gelatin type A, derived from porcine skin with ≈300 g Bloom gel strength, and 1,1,1,3,3,3-hexafluoro-2-propanol (HFIP) were purchased from Sigma-Aldrich.

2.2. Electrospun Meshes

2.2.1. Small Fiber Diameters

Viscous solutions (5%, w/v) of different weight ratios of CE-UPy-PEG/gelatin, i.e., 100/0, 90/10, 80/20, 70/30, were prepared by dissolving 200 mg solid material in 4 mL HFIP. First, the CE-UPy-PEG fraction was dissolved in HFIP, after which gelatin was added and the solutions were stirred at room temperature overnight. The clear viscous solution was transferred to a 2.5 mL glass syringes (Hamilton) and fed at 50 µL min^{-1} using a syringe pump (KR analytical) at the outside of the electrospinning cabinet to the flat-tip stainless-steel 23G needle (Intertronics) inside the cabinet, via a ≈35 cm long 1 mm I.D. poly(tetrafluoroethylene) (PTFE) tube. Inside the cabinet, each solution was spun with an in-house built electrospun setup by the application of 18.5 kV between a tip-to-target distance of 12 cm. To enable facile removal of the nonwoven electrospun mesh, the collector was covered with a thin sheet of polyethylene film. To provide a flat surface and extra support to thin samples of the electrospun mesh, fibers were collected on 12 mm round glass coverslips. The fiber deposition was interrupted several times to move the static collector plate over a 3 × 3 grid to enlarge the area of fiber deposition and to achieve a more homogeneous mesh thickness. The electrospun mesh was gently removed from the collector plate together with the polyethylene film and placed in vacuo at 40 °C to remove any residual solvent overnight.

2.2.2. Large Fiber Diameters

A more viscous solution (10%, w/v) of 80/20 CE-UPy-PEG/gelatin in HFIP was prepared by dissolving 400 mg CE-UPy-PEG and 100 mg gelatin in 5 mL HFIP and stirred at 40 °C overnight. The clear viscous solution was transferred to a syringe and connected via a 1 mm I.D. PTFE tube and a 19G needle to the climate controlled electrospinning apparatus (IME Technologies) set at 22–23 °C and 25% humidity. The solution was fed at 75 µL min^{-1}, spun by 12 kV with a tip-to-target distance of 12 cm and collected during an hour at an aluminum foil covered rotating drum with 28 mm diameter, rotating at 100 rpm. The electrospun mesh was placed in vacuo at 40 °C to remove any residual solvent overnight. The thickness of the collected CE-UPyPEG/gelatin mesh in dry state, measured with an automatic ruler, was 300 µm.

2.3. Environmental Scanning Electron Microscopy (ESEM)

ESEM imaging was performed by using FEI Quanta 600F and Xt Microscope Control software. Samples were prepared by placing small pieces of each mesh on double-sided sticky carbon tape on a metal stub. The uncoated samples were visualized under low vacuum (≈0.5 mbar) with an accelerating voltage of 15–20 kV and a working distance of 6.9–8.2 mm. Images were recorded up to 10 000 times magnification. In low vacuum, both backscattering electrons and secondary electrons were detected. Electrospun meshes with thick fibers were imaged using ESEM at high vacuum, with a voltage of 1 kV, working distance of 10 mm and spot size of 3.0 mm. Fiber diameters were determined from multiple high magnification images using ImageJ software and expressed as average ± standard deviation.

2.4. Fluorescence Microscopy Visualization of Gelatin Distribution

Prewet CE-UPy-PEG hydrogel samples on glass, both drop-cast films and electrospun meshes with varying gelatin content, were incubated overnight at 37 °C with a solution of CNA35mTurquoise2 in phosphate buffered saline (PBS) at a concentration of 1×10^{-6} M.[27] Samples were washed once with PBS before imaging with fluorescence microscopy (Zeiss Axio Observer D1) with λ_{ex} = 426–446 nm and λ_{em} = 460–500 nm.

2.5. Biaxial Mechanical Testing of Electrospun Meshes

The mechanical performances of CE-UPy-PEG electrospun meshes, both with and without gelatin, were measured. Square samples of ≈8 mm × 8 mm were cut from the meshes. The samples were weighed before and after hydration to gain insight into the swelling behavior and the thickness was determined using a digital microscope (Keyence, VHX-500F). The hydrated sample was mounted in a biaxial tensile testing device equipped with 1.5 N load cells (CellScale), as illustrated in Figure S1 (Supporting Information). Four rakes (BioRake Delicate, 0.7, 30 mm, CellScale) each consisting of five metal hooks with a diameter of 250 µm, were attached to the dry sample, leading to a 3500 µm × 3500 µm square testing area. The sample was emerged in a water bath, which was maintained at 37 °C, during the straining protocol.

For determination of elastic moduli and confirmation of isotropic behavior of the meshes with randomly oriented fibers, the meshes were cyclically loaded with three repeats of uniaxial stretch in both *x* and *y* direction, and three repeats of equibiaxial stretch. Stretch was applied at a rate of 2% s^{-1} and each final stretch was applied for 2 s. Between cycles, the sample was not loaded for 5 s to allow the fibers to relax and return to their initial configuration. The applied stretch was increased after each set of cycles starting at 10% up to 50% with increments of 10%. During the whole protocol, images were taken with a camera at a frequency of 1 Hz, while numerical data, i.e., global stretch, or displacement in micrometer and force in millinewton, was generated at a frequency of 30 Hz. The images were used as reference for visual control of sample integrity. Data were converted with Matlab (Mathworks) to calculate stresses and matched with the applied strains. In these calculations, the surface was determined by multiplying the thickness of the hydrated sample with 3500 µm, thereby assuming a uniform solid material. As the signal to noise ratio for the measured forces was low, the average stress was determined per second from the redundant data acquisition frequency. In determining the moduli via Hook's law, linear-elastic behavior of the materials was assumed. Per sample the elastic modulus was determined for both *x* and *y* direction via a linear fit through the corresponding part of the uniaxial stress–strain curve derived from a 20% or 30% stretch cyclus, upon which the average was used in determining the modulus per material.

2.6. Renal Epithelial Cell Culture

Human Kidney-2 (HK-2) cells, an immortalized proximal tubule epithelial cell line,[28] were routinely cultured in polystyrene culture flaks (BD Falcon) in complete medium consisting of Dulbecco's Modified Eagle Medium (DMEM, Gibco) supplemented with 10% heat inactivated fetal bovine serum (26140-079, Gibco, Invitrogen) and 1% penicillin-streptomycin solution (Gibco, Invitrogen), at 37 °C and 5% CO_2 in a humidified atmosphere. Cells were passed when they were 80–90% confluent. Circular samples of 12 mm, supported by a glass coverslip, were cut from the electrospun meshes (small fiber diameter). Samples were sterilized via UV-irradiation (Osram, HNS 30W G13, 13.4 W radiated power UVC 200–280 nm, with 90% of relative spectral radial power at 254 nm) for 1 h on each side at a distance of 10–20 cm, inside a lamellar airflow cabinet and fixed in dry state in minusheet tissue carriers with an outer diameter of 13 mm (Minucells and Minutissue vertriebs gmbh) or adapted transwell culture systems (BD Biosciences). The carriers with samples were placed in a 24-well tissue culture plate (BD Biosciences). Each mesh sample was submerged in an ample volume of complete medium, which was removed right before cell seeding. For low cell density, 55×10^3 HK-2 were seeded, and for high cell density, 100×10^3 HK-2 were seeded and cultured at 37 °C and

5% CO_2. The low density cell cultures were sacrificed after 1 d and actin, vincullin, and cell nuclei were stained. High cell density cultures were sacrificed after 3 d and zona occludens-1 (ZO-1) and cell nuclei were stained (see the Supporting Information).

2.7. Cardiomyocyte Progenitor Cell Culture

Cardiomyocyte progenitor cells (CMPC), immortalized via a lentiviral transduction,[29] were routinely cultured in polystyrene culture flasks precoated with 0.1% (w/v) gelatin (Sigma) in PBS. CMPC were cultured in SP++ growth medium (GM) consisting of M199 (Gibco)/EGM2 medium (3:1) supplemented with 10% fetal bovine serum, 1% penicillin/streptomycin (Lonza DE17-602E) and 1% nonessential amino acids (Gibco). CMPC were passaged when they were 80–90% confluent. Electrospun meshes with large fiber diameter were cut in circular samples with a diameter of 12 mm and sterilized via UV-irradiation (GE, NPP 130 LPF 30W G13) for 1 h on each side at a distance of 10–20 cm, inside a lamellar airflow cabinet. Meshes were then fixed in dry state in minusheet tissue carriers with an outer diameter of 13 mm (Minucells and Minutissue vertriebs gmbh). CMPC were seeded into the scaffold (250×10^3 or 1000×10^3 cells per mesh) by centrifugal force according to a previously described method.[30] Cultures were analyzed at day 1 and day 9 with Live/Dead staining or sacrificed after 1 d for immunofluorescent staining of cardiac-specific ECM components (see the Supporting Information).

3. Results and Discussion

3.1. Electrospun CE-UPy-PEG Meshes

Electrospinning of the CE-UPy-PEG polymer resulted in the formation of randomly oriented fibers with diameters typically of 0.68 ± 0.23 μm in the dry state (Figure 1B,C, state I). Upon contact with water, the white, opaque meshes hydrated and formed semitransparent hydrogel scaffolds (Figure 1B, state II). The meshes could take up over 12 times their dry weight in water (≈93 wt%). This was much more compared to the bulk CE-UPy-PEG material, which was determined to take up ≈5.7 times its dry weight in water (≈85 wt%) in equilibrated hydrated state.[19] This difference is attributed to the porous structure of the mesh. Upon hydration, the fibers swell, but also the empty spaces between them become completely filled with water as a result of capillary force. In contrast to bulk material, which swells proportionally equal in all directions, the meshes appeared to swell primarily in the height and less in the planar direction of the electrospun mesh (Figure 1B, state I and II). For individual fibers collected on a glass substrate it could be clearly observed how contact with water increased both fiber diameter and length upon hydration. Due to the high ratio between both dimensions, the proportional swelling resulted in buckling of the fibers between contact points (Figure 1B, state II and III). Hydrated samples of the mesh were dried and imaged by ESEM to gain understanding of the effect of hydration on the mesh morphology at microscale (Figure 1C, state III). Overall, the remaining fibrous structure was less well defined compared to the original dry mesh as spun. Nevertheless, contours of individual fibers could still be distinguished in the mesh. These results show that the CE-UPy-PEG polymer can be electrospun into dry solid fibrous meshes that upon exposure to aqueous solution swell into fibrous hydrogel structures. Subsequent drying of these hydrogel meshes resulted in a dry electrospun mesh, showing that the process of mesh formation, swelling and hydrogel formation, is reversible. Furthermore, degradability of CE-UPy-PEG should be addressed in future research. Due to the ethylene glycol monomers, urethane and urea functionalities, it is proposed that this mesh is prone to oxidative and enzymatic degradation in vivo.[31]

Introduction of bioactivity to the CE-UPy-PEG meshes was established by the addition of gelatin in the electrospinning solution. Mixtures with different gelatin concentrations were successfully electrospun using the same electrospinning settings and resulted in meshes with average fiber diameters of 0.68 ± 0.23 μm (0 wt% gelatin), 0.63 ± 0.36 μm (20 wt% gelatin), and 0.65 ± 0.39 μm (30 wt% gelatin) in the dry state. This indicated that the addition of gelatin to CE-UPy-PEG did not induce significant changes to the electrospinning process. In literature, increase in gelatin content has been described to reduce fiber diameters upon electrospinning by the same conditions for mixtures with various synthetic polymers, e.g., polycaprolactone,[32,33] poly(L-lactide-*co*-ε-caprolactone),[34] poly(lactic-*co*-glycolic acid),[35] and polyglycolic acid.[36] However, up to 30 wt% gelatin could be added to CE-UPy-PEG while maintaining similar mesh morphology and swelling behavior.

3.2. Mechanical Testing

Elasticity and durability of a hydrogel scaffold is of high importance in for example cardiovascular tissue engineering applications, which involve mechanical loading under cyclic loading. The mechanical properties of electrospun scaffolds are highly dependent on the processing parameters. Next to polymeric composition, also fiber diameter and orientation are major factors that determine the elastic modulus of electrospun meshes.[32] To gain understanding of the mechanical properties of electrospun CE-UPy-PEG, hydrated meshes were subjected to biaxial tensile tests (Figure S1, Supporting Information). The effect of gelatin was determined by comparison of meshes of CE-UPy-PEG with 0, 20, and 30 wt% gelatin (**Figure 2**A). As expected, the random orientation of the fibers in these meshes, resulted in isotropic elastic behavior in x and y direction (Figure S2, Supporting Information). Furthermore, stress–strain curves of meshes which were stretched and relaxed in the x direction showed overlap, which indicates minimal plastic deformation within the applied range of strains (Figure 2B). Elastic moduli were determined for pure CE-UPy-PEG meshes, and hybridized meshes with 20% and 30% gelatin (**Table 1**). Initial measurements did not reveal an influence of the addition of gelatin on the mechanical properties of the meshes. All hydrogel meshes exhibited strain-to-failure of at least 40%. At higher deformations, the material started to tear at the points where the mesh was punctured with thin metal pins for attachment to the biaxial tensile testing device. When strains were further increased, eventually total rupture always occurred along a row of these pins. At these points in the material, locally higher stresses occur. Therefore, the currently derived elastic moduli are probably underestimates as these were derived from global stress–strain curves. However the strain-to-failure could be considered representative for applications that require for example suturing of the hydrogel meshes. These results indicate that CE-UPy-PEG-based hydrogel

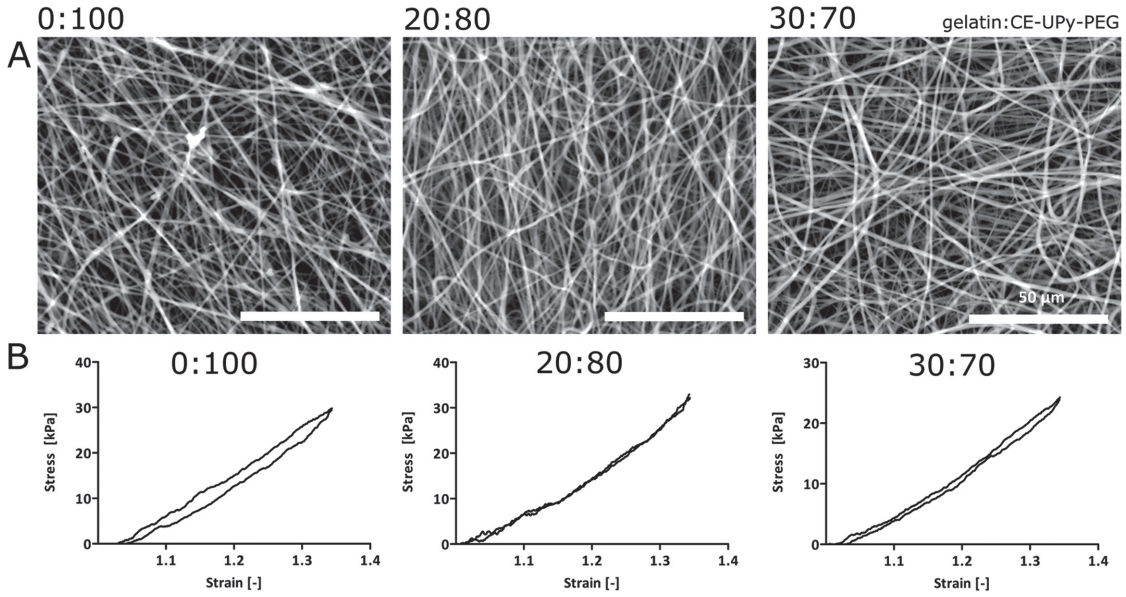

Figure 2. Electrospun CE-UPy-PEG with gelatin and mechanical testing of electrospun hydrogel meshes. A) Scanning electron micrographs of dry electrospun meshes of CE-UPy-PEG with 0, 20, and 30 wt% gelatin. The scale bars indicate 50 µm. B) Uniaxial stress–strain graphs showing one stretch-relax cycle of electrospun hydrogel meshes of CE-UPy-PEG with 0, 20, and 30 wt% gelatin in wet-state.

meshes could potentially be applied in tissue engineering applications that involve mechanical straining up to 30–40%.

3.3. Renal Epithelial Cell Adhesion and Monolayer Formation

Renal epithelial cells did not adhere to drop-cast films solely consisting of CE-UPy-PEG owing to the antifouling nature of PEG. The addition of gelatin to CE-UPy-PEG in the drop-cast process only resulted in minor improvement of cell adhesion, which is proposed to occur due to inhomogeneous mixing of gelatin into the CE-UPy-PEG (Figures S3–S5, Supporting Information). However, when a mixed solution of CE-UPy-PEG and gelatin was processed by electrospinning, gelatin was homogeneously distributed throughout each mesh (**Figure 3**A). Cells were first seeded in subconfluent densities on these meshes to enable focus on cell–biomaterial interactions rather than cell–cell interactions. Cell adhesion was improved upon introduction of gelatin in the electrospun mesh. Interestingly, formation of focal adhesions by attached renal epithelial cells was identified via vinculin rich spots 1 d after cell seeding (Figure S6, Supporting Information). The formation of focal adhesions provides evidence for the interaction between cells and the hybrid mesh. This thus confirmed the presence of the gelatin at the fibers surface and successful incorporation of bioactivity through the use of gelatin in combination with electrospinning.

In order to create a tissue engineered renal cell monolayer, which can possibly be translated toward an artificial kidney application,[37] higher densities of renal epithelial cells were used. The adhered cells were allowed to mature for 3 d prior to evaluation of their morphology by fluorescence microscopy (Figure 3B). The presence of 10 wt% gelatin in the CE-UPy-PEG mesh allowed some renal epithelial cells to adhere and grow in a patchy conformation. In presence of 20 and 30 wt% gelatin, the renal epithelial cells formed a near confluent layer (Figure 3B). Staining of zona occludens-1 (ZO-1) protein and visualization by fluorescence microscopy revealed the presence of tight junctions between the cells (Figure 3C). This points toward the formation of a tight renal epithelial cell layer on this hybrid hydrogel mesh. These results suggest suitability of the hybridized microfibrous hydrogels to function as scaffold to support the formation of a confluent and functional renal cell monolayer.

3.4. CMPC Viability and Extracellular Matrix Production

Hybrid hydrogel meshes with a more open pore structure were hypothesized to provide a suitable 3D environment for CMPC.

Table 1. Elastic moduli of electrospun CE-UPy-PEG hydrogel meshes, with and without gelatin.

CE-UPy-PEG/gelatin ratio	Number of samples	Average fiber diameter [µm]	Average thickness[a] [µm]	Average E modulus[b] [MPa]
100/0	$N = 3$	0.68 ± 0.23	459 ± 36	0.64 ± 0.19
80/20	$N = 3$	0.63 ± 0.36	374 ± 51	0.60 ± 0.15
70/30	$N = 2$	0.65 ± 0.39	519 ± 141	0.61 ± 0.06

[a]Thickness of hydrated samples; [b]Elastic moduli were determined as the slope of the linear range of stress-strain curves.

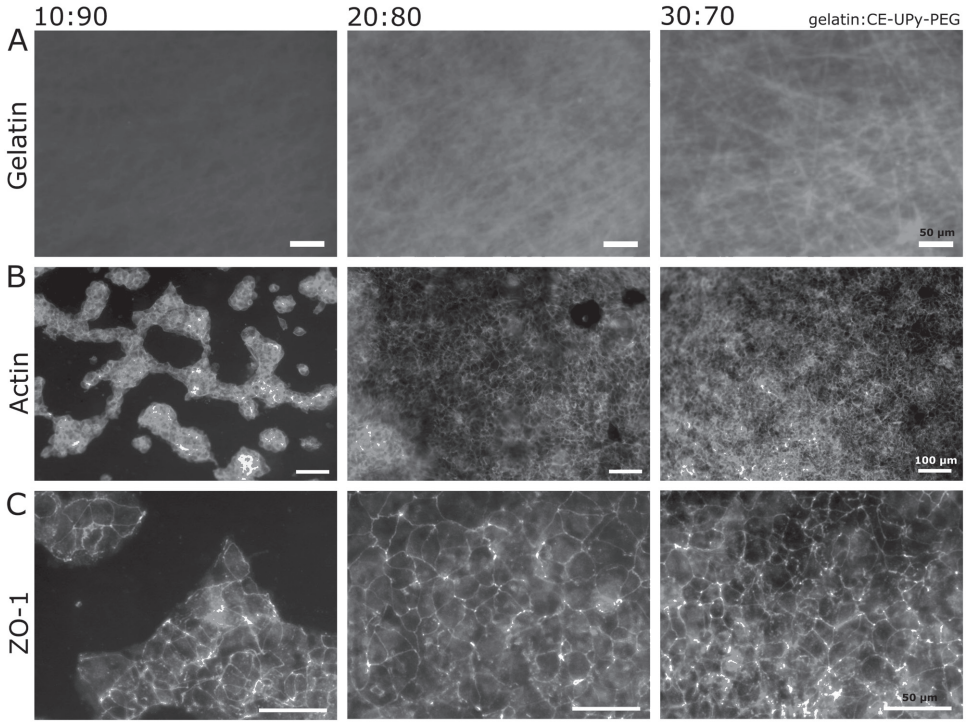

Figure 3. HK-2 adhesion and monolayer formation on electrospun hybrid meshes. A) Fluorescence micrographs show the location of fluorescently stained gelatin in hydrated electrospun meshes of CE-UPy-PEG with 10, 20, and 30 wt% gelatin. Scale bars indicate 50 µm. B) Fluorescence micrographs show intracellular actin of HK-2 cells 3 d after seeding on electrospun meshes of CE-UPy-PEG with 10, 20, and 30 wt% gelatin. Scale bars indicate 100 µm. C) Immunofluorescence micrographs show cell–cell interactions with ZO-1 of HK-2 cells 3 d after seeding on electrospun meshes of CE-UPy-PEG with 10, 20, and 30 wt% gelatin. Scale bars indicate 50 µm.

The function of such a hydrogel is to maintain cell viability and support growth and differentiation. It should hence act as a temporarily 3D microenvironment which resembles the native niche until the cells have formed their own ECM. Electrospinning a concentrated (10%, w/v) solution of 80%/20% (w/w) CE-UPy-PEG/gelatin resulted in a mesh with average fiber diameters of 2.14 ± 0.63 µm and apparent pore sizes bigger than 10 µm (**Figure 4**A). Next, CMPC were seeded inside the open porous structure of electrospun CE-UPy-PEG/gelatin meshes. To actively aid cell infiltration, cells were forced into

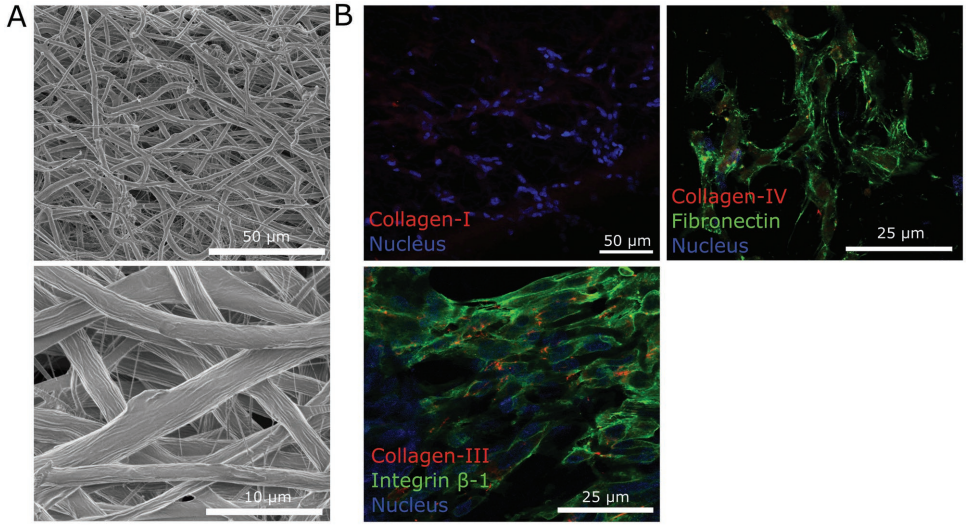

Figure 4. Electrospun CE-UPy-PEG meshes and ECM production of CMPC inside electrospun hybrid meshes. A) Scanning electron micrographs of an electrospun scaffold prepared from a concentrated solution (10%, w/v) of CE-UPy-PEG with 20 wt% gelatin. B) Immunofluorescence confocal micrographs show ECM production of CMPC after 1 d in the electrospun meshes. Collagen I, collagen IV, and collagen III are represented in red, integrin-β1, and fibronectin are represented in green and CMPC nuclei are represented in blue.

the mesh by centrifugation. Cell infiltration depth in the hybrid CE-UPy-PEG/gelatin mesh increased after application of centrifugal force compared to static seeding, with depths of 69 and 20 μm, respectively (Figure S7, Supporting Information).

The viability of CMPC after 1 d of seeding was 97.5 ± 0.5% and after 9 d, cell viability slightly decreased to 93.2 ± 2.2% (Figure S8, Supporting Information). This is due to the thin electrospun meshes (300 μm in dry state), which allows for sufficient oxygen and nutrient to the cells. In addition, the deposition of cardiac-specific ECM proteins by CMPC was determined by immunofluorescent staining for collagen I, III, IV, and fibronectin (Figure 4B). After 1 d of culturing inside the hydrogel mesh, CMPC produced limited amounts of cytoplasmic collagen I and IV. Costaining of collagen III and membrane marker integrin β1 revealed the presence of collagen III in the extracellular space. Furthermore, high amounts of fibronectin were produced after 1 d. This fibronectin formed a fibrous structure at the attachment points with the scaffold. One of the hurdles of hybrid hydrogels composed of a synthetic and natural component is that the biological ECM component often degrades more rapid than its replacement which is secreted by cells. Therefore, the deposition of ECM proteins by CMPC shown here, is proposed to provide a promising start for successful long-term outcome.

4. Conclusions

These results show that hybrid hydrogel meshes based on CE-UPy-PEG can function as a robust free-standing scaffold and support the formation of a renal cell monolayer and act as a cardiac niche by simply tuning the fiber diameter. CE-UPy-PEG was successfully processed by electrospinning into relevant fibrous morphologies, which are stable under physiological conditions without the need of chemical crosslinking. The combination with gelatin demonstrates the possibility to make hybrid scaffolds with natural bioactive proteins, while synthetic UPy-peptide based approaches toward more specific and controlled bioactivation might be explored in the future.[38,39] The elastic behavior of the hydrogel scaffolds and durability under cyclic loading widens the scope of possible tissue engineering applications.

Supporting Information

Supporting Information is available from the Wiley Online Library or from the author.

Acknowledgements

Anthal Smits is acknowledged for his support and guidance in the mechanical analysis of the hybrid hydrogel meshes. Louis Pitet is thanked for the synthesis of the CE-UPy-PEG polymer. Marie-José Goumans is gratefully acknowledged for the L9TB CMPC. The research leading to these results received funding from the ministry of Education, Culture, and Science (Gravity program 024.001.035), The Netherlands Organization for Scientific Research (NWO), the European Research Council (FP7/2007-2013), ERC Grant Agreement No. 308045. This research forms part of the Project P3.01 BioKid of the research program of the Biomedical Materials institute, cofounded by the Dutch Ministry of Economic Affairs. The financial contribution of the Dutch Kidney Foundation is gratefully acknowledged. Also, this research forms part of the Cardiovascular Onderzoek Nederland (CVON). The financial contribution of the Nederlandse Hartstichting is gratefully acknowledged.

Conflict of Interest

The authors declare no conflict of interest.

Keywords

electrospun meshes, hybrid hydrogels, mechanical properties, supramolecular biomaterials, tissue engineering

Received: February 10, 2017
Revised: May 16, 2017
Published online:

[1] R. M. Wang, K. L. Christman, *Adv. Drug Delivery Rev.* **2016**, *96*, 77.
[2] M. van Marion, N. Bax, A. van Spreeuwel, D. van der Schaft, C. Bouten, *Curr. Pharm. Des.* **2014**, *20*, 12.
[3] C. V. C. Bouten, P. Y. W. Dankers, A. Driessen-Mol, S. Pedron, A. M. A. Brizard, F. P. T. Baaijens, *Adv. Drug Delivery Rev.* **2011**, *63*, 4.
[4] J. L. Drury, D. J. Mooney, *Biomaterials* **2003**, *24*, 4337.
[5] B. V. Slaughter, S. S. Khurshid, O. Z. Fisher, A. Khademhosseini, N. A. Peppas, *Princ. Regener. Med.* **2011**, *21*, 3307.
[6] J. Radhakrishnan, U. M. Krishnan, S. Sethuraman, *Biotechnol. Adv.* **2014**, *32*, 2.
[7] C. S. Hughes, L. M. Postovit, G. a. Lajoie, *Proteomics* **2010**, *10*, 1886.
[8] H. K. Kleinman, G. R. Martin, *Semin. Cancer Biol.* **2005**, *15*, 378.
[9] X. Jia, K. L. Kiick, *Macromol. Biosci.* **2009**, *9*, 2.
[10] J. Zhu, R. E. Marchant, *Expert Rev. Med. Devices* **2011**, *8*, 5.
[11] F. Anjum, A. Carroll, S. A. Young, L. E. Flynn, B. G. Amsden, *Macromol. Biosci.* **2017**, *17*, 1600373.
[12] J. A. Matthews, G. E. Wnek, D. G. Simpson, G. L. Bowlin *Biomacromolecules* **2002**, *3*, 2.
[13] L. Liu, M. Yoshioka, M. Nakajima, A. Ogasawara, J. Liu, K. Hasegawa, S. Li, J. Zou, N. Nakatsuji, K. i. Kamei., Y. Chen, *Biomaterials* **2014**, *35*, 24.
[14] J. S. Im, J. Yun, Y. M. Lim, H. Il, S. Y. Lee Kim, *Acta Biomater.* **2010**, *6*, 1.
[15] J. S. Stephens-Altus, P. Sundelacruz, M. L. Rowland, J. L. West, *J. Biomed. Mater. Res., Part A* **2011**, *98*, 2.
[16] A. Gestos, P. G. Whitten, G. G. Wallace, G. M. Spinks, *Soft Matter* **2012**, *8*, 31.
[17] A. Cay, M. Mohsen, *J. Appl. Polym. Sci.* **2013**, *129*, 6.
[18] K.-O. Kim, Y. Akada, W. Kai, B.-S. Kim, I.-S. Kim, *J. Biomater. Nanobiotechnol.* **2011**, *2*, 4.
[19] M. Guo, L. M. Pitet, H. M. Wyss, M. Vos, P. Y. W. Dankers, E. W. Meijer, *J. Am. Chem. Soc.* **2014**, *136*, 19.
[20] P. Y. W. Dankers, T. M. Hermans, T. W. Baughman, Y. Kamikawa, R. E. Kieltyka, M. M. C. Bastings, H. M. Janssen, N. A. J. M. Sommerdijk, A. Larsen, M. J. A. van Luyn, A. W. Bosman, E. R. Popa, G. Fytas, E. W. Meijer, *Adv. Mater.* **2012**, *24*, 20.
[21] M. M. C. Bastings, S. Koudstaal, R. E. Kieltyka, Y. Nakano, A. C. H. Pape, D. A. M. Feyen, F. J. van Slochteren,

P. A. Doevendans, J. P. G. Sluijter, E. W. Meijer, S. A. J. Chamuleau, P. Y. W. Dankers, *Adv. Healthcare Mater.* **2014**, *3*, 1.
[22] R. E. Kieltyka, A. C. H. Pape, L. Albertazzi, Y. Nakano, M. M. C. Bastings, I. K. Voets, P. Y. W. Dankers, E. W. Meijer, *J. Am. Chem. Soc.* **2013**, *135*, 30.
[23] A. C. H. Pape, M. M. C. Bastings, R. E. Kieltyka, H. M. Wyss, I. K. Voets, E. W. Meijer, P. Y. W. Dankers, *Int. J. Mol. Sci.* **2014**, *15*, 1.
[24] D. I. Zeugolis, S. T. Khew, E. S. Y. Yew, A. K. Ekaputra, Y. W. Tong, L. Y. L. Yung, D. W. Hutmacher, C. Sheppard, M. Raghunath, *Biomaterials* **2008**, *29*, 15.
[25] Z. M. Huang, Y. Z. Zhang, S. Ramakrishna, C. T. Lim, *Polymer* **2004**, *45*, 15.
[26] S. Zhang, Y. Huang, X. Yang, F. Mei, Q. Ma, G. Chen, S. Ryu, X. Deng, *J. Biomed. Mater. Res. A* **2009**, *90*, 671.
[27] S. J. A. Aper, A. C. C. Van Spreeuwel, M. C. Van Turnhout, A. J. Van Der Linden, P. A. Pieters, N. L. L. Van Der Zon, S. L. De La Rambelje, C. V. C. Bouten, M. Merkx, *PLoS One* **2014**, *9*, e114983.
[28] M. J. Ryan, G. Johnson, J. Kirk, S. M. Fuerstenberg, R. A. Zager, B. Torok-Storb, *Kidney Int.* **1994**, *45*, 1.
[29] A. M. Smits, P. van Vliet, C. H. Metz, T. Korfage, J. P. G. Sluijter, P. A. Doevendans, M.-J. Goumans, *Nat. Protoc.* **2009**, *4*, 2.
[30] A. E. Ghalbzouri, E. Lamme, M. Ponec, *Cell Tissue Res.* **2002**, *310*, 189.
[31] M. B. Browning, S. N. Cereceres, P. T. Luong, E. M. J. Cosgriff-Hernandez, *Biomed. Mater. Res., Part A* **2014**, *102*, 4244.
[32] E. Vatankhah, D. Semnani, M. P. Prabhakaran, M. Tadayon, S. Razavi, S. Ramakrishna, *Acta Biomater.* **2014**, *10*, 2.
[33] L. Ghasemi-Mobarakeh, M. P. Prabhakaran, M. Morshed, M.-H. Nasr-Esfahani, S. Ramakrishna, *Biomaterials* **2008**, *29*, 34.
[34] J. Lee, G. Tae, Y. H. Kim, I. S. Park, S. H. Kim, S. H. Kim, *Biomaterials* **2008**, *29*, 12.
[35] Z. X. Meng, Y. S. Wang, C. Ma, W. Zheng, L. Li, Y. F. Zheng, *Mater. Sci. Eng. C* **2010**, *30*, 8.
[36] H. Hajiali, S. Shahgasempour, M. R. Naimi-Jamal, H. Peirovi, *Int. J. Nanomed.* **2011**, *6*, 2133.
[37] P. Y. W. Dankers, J. M. Boomker, A. Huizinga-van der Vlag, E. Wisse, W. P. J. Appel, F. M. M. Smedts, M. C. Harmsen, A. W. Bosman, W. Meijer, M. J. A. van Luyn, *Biomaterials* **2011**, *32*, 3.
[38] B. B. Mollet, M. Comellas-Aragonès, A. J. H. Spiering, S. H. M. Söntjens, E. W. Meijer, P. Y. W. Dankers, *J. Mater. Chem. B* **2014**, *2*, 17.
[39] D. E. P. Muylaert, G. C. van Almen, H. Talacua, J. O. Fledderus, J. Kluin, S. I. S. Hendrikse, J. L. J. van Dongen, E. Sijbesma, A. W. Bosman, T. Mes, S. H. Thakkar, A. I. P. M. Smits, C. V. C. Bouten, P. Y. W. Dankers, M. C. Verhaar, *Biomaterials* **2016**, *76*, 187.

